

# Fluctuation-Dissipation Relations and statistical temperatures in a turbulent von Kármán flow

Romain Monchaux,<sup>1</sup> Pierre-Philippe Cortet,<sup>1</sup> Pierre-Henri Chavanis,<sup>2</sup> Arnaud Chiffaudel,<sup>1</sup> François Daviaud,<sup>1</sup> Pantxo Diribarne,<sup>1</sup> and Bérengère Dubrulle<sup>1</sup>

<sup>1</sup>*Service de Physique de l'État Condensé, DSM, CEA Saclay, CNRS URA 2464, 91191 Gif-sur-Yvette, France*

<sup>2</sup>*Laboratoire de Physique Théorique, CNRS UMR 5152,*

*Université Paul Sabatier, 118 route de Narbonne, 31062 Toulouse, France*

We experimentally characterize the fluctuations of the non-homogeneous non-isotropic turbulence in an axisymmetric von Kármán flow. We show that these fluctuations satisfy relations, issued from the Euler equation, which are analogous to classical Fluctuation-Dissipation Relations in statistical mechanics. We use these relations to estimate statistical temperatures of turbulence.

PACS numbers: 47.27.E-, 05.70.Ln

Fluctuation-Dissipation Relations (FDRs) are one of the corner-stone of statistical mechanics. They offer a direct relation between the fluctuations of a system at equilibrium and its response to a small external perturbation. Classical outcome of FDRs are Einstein or Nyquist relations, or, more generally, measures of the susceptibility, dissipation coefficient or temperature of the system. The hypothesis behind the FDRs restrict their applicability to systems that are close to equilibrium. Theoretical extrapolation of the FDRs to systems far from equilibrium is currently a very active area of research [1]. In this context, experimental tests in several glassy systems have evidenced violation of FDRs [2]. Furthermore, general identities about fluctuations and dissipation, theoretically derived for time-symmetric out of equilibrium systems [3], have been tested in dissipative (non time-symmetric) systems like electrical circuit or turbulent flow [4]. Turbulence is actually a very special example of far from equilibrium system. Due to its intrinsic dissipative nature, an unforced turbulent flow is bound to decay to rest. However, in the presence of a permanent forcing, a steady state regime can be established, in which forcing and dissipation equilibrate on average, allowing the maintenance of non-zero averaged velocities, with large fluctuations covering a wide range of scales. We use measurements performed in a turbulent von Kármán flow to show that there is actually a direct link between these fluctuations and the mean flow properties, in a way analogous to classical FDRs. This approach provides an estimate of effective statistical temperatures of our turbulent flow.

*Theoretical background and definitions.*- Describing turbulence with tools borrowed from statistical mechanics is a long-standing dream, starting with Onsager [5]. Advances in that direction have been recently made for flows with symmetries (2D [6], axisymmetric [7]) using tools developed independently by Robert and Sommeria and Miller [8]. They consider freely evolving flows described by the Euler equation (no forcing and no dissipation). The Euler equation conserves the energy and,

for axisymmetric and shear flows, the helicity. In addition, owing to the symmetry, there is conservation of a local scalar quantity along a velocity line (vorticity in 2D, angular momentum for axisymmetry) resulting in a Liouville theorem and additional global conserved quantities as Casimirs of the local scalar quantity. In the Miller-Robert-Sommeria theory, the Euler equation develops a mixing process leading to a quasi-stationary state on the coarse-grained scale. This state is determined by the initial conditions and maximizes a mixing entropy under conservation of all the inviscid invariants. For forced dissipative flows, the strict conservation of the inviscid invariants is lost. However, an equilibrium between forcing and dissipation can establish itself and the system can reach a steady state that is a combination of a stationary solution of the Euler equation and fluctuations. This steady state is selected by forcing and dissipation. Some authors [6, 9] have proposed to describe this state by maximizing a mixing entropy under only particular constraints (see for example  $H_f$  and  $I_g$  in Eq. 1) selected implicitly by forcing and dissipation. This allows the derivation of Gibbs states of the system from which one derives general identities characterizing the steady states, as well as relations between these steady states and their fluctuations.

We apply this approach to the axisymmetric case which is relevant to our experimental device. In that case, the variables describing the system are the angular momentum  $\sigma$ , the stream function  $\psi$  and the rescaled azimuthal vorticity  $\xi = r^{-1}\omega_\theta$  [7, 10]. The representation of the flow through  $(\sigma, \psi, \xi)$  or through the classical velocity components  $(u_r, u_\theta, u_z)$  in cylindrical coordinates  $(r, \theta, z)$  are equivalent since  $(u_r, 0, u_z) = \nabla \times (r^{-1}\psi \mathbf{e}_\theta)$  and  $u_\theta = \sigma/r$ . Furthermore,  $r^{-1}\partial_r(r^{-1}\partial_r\psi) + r^{-2}\partial_z^2\psi = -\xi$ . In the inviscid, force-free limit, the global quantities conserved by the Euler equation are the energy  $E$ , the generalized helicities  $H_f$  and the Casimirs  $I_g$ , given by [7]:

$$E = \frac{1}{2} \int \xi \psi r dr dz + \frac{1}{2} \int \frac{\sigma^2}{r^2} r dr dz,$$

$$H_f = \int \xi f(\sigma) r dr dz, \quad I_g = \int g(\sigma) dy dz, \quad (1)$$

where  $f$  and  $g$  are arbitrary functions. For forced dissipative flows, it has been suggested to conserve only the energy  $E$  and two particular integrals  $H_f$  and  $I_g$  where the functions  $f$  and  $g$  are selected through forcing and dissipation [10]. For Beltrami flows, in which vorticity is proportional to velocity everywhere, i.e.  $\mathbf{u} = \lambda \nabla \times \mathbf{u}$ , the relevant conserved quantities are the energy  $E$  and the helicity  $H$  so that  $f(\sigma) = \sigma$  and  $g = 0$  [7].

Let us now apply the statistical mechanics approach introduced in the previous paragraph to a Beltrami flow. The detailed procedure is described in [7, 11]. The mixing entropy of the flow  $S[\rho]$  is defined using the probability density  $\rho(\sigma, \xi, \mathbf{r})$  to have a certain couple of values for  $\sigma$  and  $\xi$  at each position  $\mathbf{r}$ . Because of the Beltrami hypothesis, the steady state of the flow maximizes  $S[\rho]$  at fixed energy  $E$  and helicity  $H$ . Then, writing  $\delta S - \beta \delta E - \mu \delta H = 0$  (where  $\beta^{-1}$  is a temperature and  $\mu$  an ‘‘helical potential’’) and using two different mean field approximations, one finds two relations for the averaged fields[14]:

$$\beta_\xi \bar{\psi} + \mu_\xi \bar{\sigma} = 0, \quad (2a)$$

$$\frac{\beta_\sigma \bar{\sigma}}{r^2} + \mu_\sigma \bar{\xi} = 0, \quad (2b)$$

as well as two expressions for the probability density  $\rho_\xi(\sigma, \mathbf{r})$  and  $\rho_\sigma(\xi, \mathbf{r})$ , which happen to be Gaussian functions. The two mean field approximations consist in fixing independently  $\xi$  or  $\sigma$  to their time average. The thermodynamic coefficients  $\mu$  and  $\beta$  have been labelled accordingly. Considering the first moment of  $\rho_\xi$ , one gets an additional relation for the averaged fields:

$$\frac{\beta_\xi \bar{\sigma}}{r^2} + \mu_\xi \bar{\xi} = 0. \quad (3)$$

Finally, considering the second moment of  $\rho_\xi(\sigma, \mathbf{r})$  and  $\rho_\sigma(\xi, \mathbf{r})$ , we obtain relations for fluctuations:

$$\overline{\sigma^2} - \bar{\sigma}^2 = \frac{r^2}{\beta_\xi}, \quad \overline{\xi^2} - \bar{\xi}^2 = \frac{\beta_\sigma}{\mu_\sigma^2 r^2}. \quad (4)$$

Comparing Eq. (2b) with Eq. (3), we see that the four thermodynamic coefficients in these equations obey:

$$\frac{\mu_\sigma}{\beta_\sigma} = \frac{\mu_\xi}{\beta_\xi}. \quad (5)$$

Dividing Eq. (2a) by  $r$  and taking its curl, we obtain a relation between the poloidal components, i.e. the components in  $r$ - $z$  plane, of the velocity and vorticity:  $\overline{\mathbf{u}_p} = -\mu_\xi/\beta_\xi \overline{\boldsymbol{\omega}_p}$ . Then, multiplying Eq. (2b) by  $r$ , we obtain the following relation for the toroidal, i.e. azimuthal, components:  $\overline{u_\theta} = -\mu_\sigma/\beta_\sigma \overline{\omega_\theta}$ . Finally, using Eq. (5), we get:

$$\overline{\mathbf{u}} = -\frac{\mu_\sigma}{\beta_\sigma} \nabla \times \overline{\mathbf{u}}, \quad (6)$$

and verify that the averaged flow is a Beltrami flow with a constant  $\lambda = -\mu_\sigma/\beta_\sigma = -\mu_\xi/\beta_\xi$ . Note that this flow minimizes the coarse-grained energy at fixed helicity. Additionally, combining Eqs. (2a) and (2b), we find that:

$$\overline{\mathbf{u}_p} = \frac{\mu_\sigma}{\beta_\sigma} \frac{\mu_\xi}{\beta_\xi} \nabla \times (\overline{\boldsymbol{\omega}_\theta} \mathbf{e}_\theta) = \lambda^2 \nabla \times (\overline{\boldsymbol{\omega}_\theta} \mathbf{e}_\theta), \quad (7)$$

namely that a spatial variation of the azimuthal vorticity creates a poloidal velocity with a proportionality constant  $\lambda^2$ . This relation can be used to define a susceptibility  $\chi \equiv 1/\lambda^2$  which happens to be always positive.

Eqs. (4) can easily be recast into:

$$\overline{u_\theta^2} - \bar{u}_\theta^2 = \frac{1}{\beta_\xi}, \quad (8a)$$

$$\overline{\omega_\theta^2} - \bar{\omega}_\theta^2 = \frac{\chi}{\beta_\sigma}, \quad (8b)$$

predicting uniformity of azimuthal velocity and vorticity fluctuations. Eq. (8a) shows that the azimuthal velocity fluctuations define an effective statistical temperature  $1/\beta_\xi$ . Eq. (8b) links the vorticity fluctuations to the susceptibility  $\chi$  and a vortical effective temperature  $1/\beta_\sigma$ . This is a formal equivalent of the Einstein relation for the Brownian motion. These equations may be regarded as formally analogous to FDRs since they link fluctuations, susceptibility and temperature. These predictions enable the measurements of turbulence effective temperatures through fluctuations of  $u_\theta$  and  $\omega_\theta$  in a Beltrami flow. Because variances are positive,  $\beta_\sigma$  and  $\beta_\xi$  are always positive (since  $\chi > 0$ ), unlike in the 2D situation where  $\chi$  can be negative [15]. In contrast,  $\mu_\sigma$  and  $\mu_\xi$  can take positive or negative values, depending on the helicity sign.

The analogy between our predictions and FDRs can actually be pushed forward. An other possible way to derive Eqs. (4) is to introduce, as in classical statistical mechanics, the partition function  $Z_{\xi, \sigma}$  describing the Beltrami equilibrium state in each mean field approximation:

$$\overline{\sigma^2} - \bar{\sigma}^2 = \frac{1}{\mu_\xi^2} \frac{\delta^2 \log Z_\xi}{\delta \bar{\xi}^2} = -\frac{1}{\mu_\xi} \frac{\delta \bar{\sigma}}{\delta \bar{\xi}}, \quad (9a)$$

$$\overline{\xi^2} - \bar{\xi}^2 = \frac{1}{\mu_\sigma^2} \frac{\delta^2 \log Z_\sigma}{\delta \bar{\sigma}^2} = -\frac{1}{\mu_\sigma} \frac{\delta \bar{\xi}}{\delta \bar{\sigma}}. \quad (9b)$$

Formally, the mathematical objects  $\delta \bar{\sigma}/\delta \bar{\xi}$  and  $\delta \bar{\xi}/\delta \bar{\sigma}$  can be seen as response functions. With this point of view, Eqs. (9) again reflect a formal analogy with FDRs since another classical way to write it down is to link the fluctuations of a field to its response to a perturbation.

The challenge is to face such fluctuation relations with experimental data. For this, we use a turbulent von Kármán flow that has already been shown to tend to a Beltrami flow at large Reynolds number [10].

*Experimental flow and measurement techniques.*— Our experimental setup consists of a plexiglas cylinder (radius  $R_c = 100$  mm) filled up with water. The fluid is

mechanically stirred by a pair of impellers driven by two independent motors in exact counterrotation. The resulting flow belongs to the von Kármán class of flows with a mean flow divided into two toric cells separated by an azimuthal shear layer. We define the Reynolds number as  $Re = UL/\nu = 2\pi FR_c^2/\nu$ , where  $F$  is the impeller frequency and  $\nu$  the water viscosity. Rotating the impellers from 125,000 to 500,000. Our two models of impellers, TM60 and TM73, are flat disks of respective radius  $0.925 R_c$  and  $0.75 R_c$ , fitted with radial blades of height  $0.2 R_c$  and respective curvature  $0.50 R_c$  and  $0.925 R_c$ . The inner face of the discs are  $1.8 R_c$  apart. Different forcings are associated with the convex or concave face of the blades going forward, denoted in the sequel by senses (+) and (-). Velocity measurements are done with a Stereoscopic Particle Image Velocimetry system [11] provided by DANTEC Dynamics. The cylinder is mounted inside a water filled square plexiglas container in order to reduce optical deformations. Two digital cameras are aiming at a meridian plane of the flow through two perpendicular faces of the square container giving a 2D-three components velocity field map. Correlation calculations are done on  $32 \times 32$  pixels<sup>2</sup> windows with 50% overlap. As a result, each velocity is averaged on a  $4.16 \times 4.16$  mm<sup>2</sup> window over the 1.5 mm laser sheet thickness. The spatial resolution is 2.08 mm. A basic measurement is a set of 5000 acquisitions at a rate of 4 images per second. From this set, we compute time-average and fluctuations of the three velocity components.

From now on, all physical quantities and equations will be considered in their non-dimensionalized form using  $F$  and  $R_c$ . For each of the four forcing configurations, we made between five and seven tests that show no  $Re$ -dependency for these non-dimensionalized quantities.

*Test of the mean flow relations.*- Relations (2a) and (2b) can be tested by plotting  $\bar{\psi}$  and  $\bar{\xi}r^2$  with respect to  $\bar{\sigma}$  for each experiment. Two of them are plotted in Fig. 1. As in Ref. [10], we focus on the flow bulk, i.e.  $|z| \leq 0.5$  and  $|r| \leq 0.5$ , where the von Kármán flow is close to a Beltrami flow. Linear dependencies of Eqs. (2) are confirmed [10] and enable estimation of the slopes  $\beta_\sigma/\mu_\sigma$  and  $\beta_\xi/\mu_\xi$  (see caption of Fig. 1 for details and Table I for averaged results). Depending on the forcing, the two measurements of  $\beta/\mu$  differ from 1 to 13%, verifying Eq. (5) and giving a unique mean value of  $\beta/\mu$  or  $\lambda$  (see Table I, line 3). The quality of the test of Eq. (5) is evaluated by  $\beta_\xi/\mu_\xi - \beta_\sigma/\mu_\sigma$  (line 4). One can see that the two 68% confidence intervals of  $\beta_\xi/\mu_\xi$  and  $\beta_\sigma/\mu_\sigma$  always overlap.

*Test of the fluctuation relations.*- Now, we turn to experimental test of fluctuation relations (8) and to complete determination of the four *a priori* independent coefficients:  $\beta_\xi$ ,  $\beta_\sigma$ ,  $\mu_\xi$  and  $\mu_\sigma$ . Because of Eq. (5), only three of them are independent and the previous test already provided a measurement of  $\beta/\mu$ . So, we can use

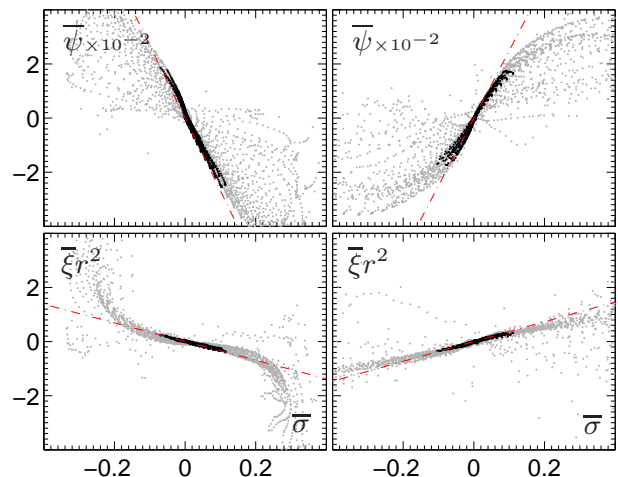


FIG. 1:  $\bar{\psi}$  (top) and  $\bar{\xi}r^2$  (bottom) versus  $\bar{\sigma}$  for two experimental von Kármán flow with TM60 impellers at  $F = 6$ Hz, sense (+) at left, (-) at right. Black dots correspond to flow bulk data ( $|z| \leq 0.5$ ,  $|r| \leq 0.5$ ) and define mostly linear functions. The slopes of the dot-dashed lines is given by the first order coefficient of an odd cubic fit of the data. Corresponding values of  $\beta_\sigma/\mu_\sigma$  and  $\beta_\xi/\mu_\xi$  are used to compute Table I.

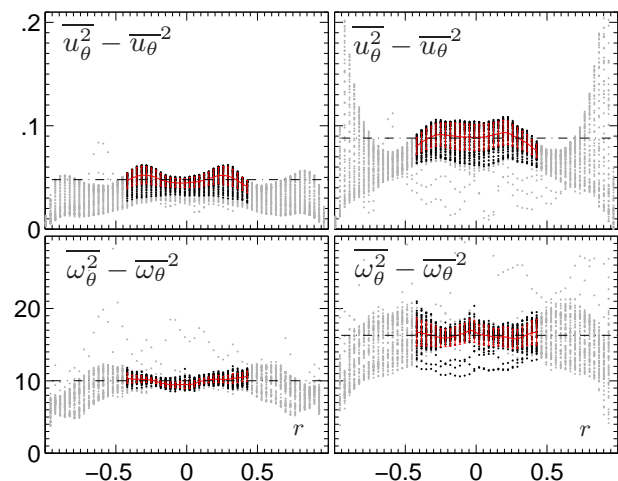


FIG. 2: Evolution of angular velocity fluctuations (top) and angular momentum fluctuations (bottom) with the radial coordinate  $r$  for the same flows as in Fig. 1. Black dots correspond to flow bulk data ( $|z| \leq 0.5$ ,  $|r| \leq 0.5$ ). The corresponding mean values and standard deviations at each  $z$  are plotted by red lines and errorbars. Horizontal dot-dashed lines show the averages over the flow bulk, i.e. measured values for  $1/\beta_\xi$  and  $\beta_\sigma/\mu_\sigma^2$ .

the fluctuation relations of Eqs. (8) to compute the remaining parameters  $1/\beta_\xi$  and  $\beta_\sigma/\mu_\sigma^2$ .

Fig. 2 presents the analysis of the fluctuation relations for angular velocity  $u_\theta$  and vorticity  $\omega_\theta$ . On the top plots, we test relation (8a). Over the whole flow, the velocity fluctuations are roughly constant. The relative scattering, which mostly tracks the  $z$ -dependance, increases with  $r$ . Focusing again on the flow bulk, we observe a reduced scattering and measure  $1/\beta_\xi$  with a simple average. On the bottom plots, we perform the same analysis for vorticity fluctuations and relation (8b). The

Impellers	TM73		TM60	
Sense	(+)	(-)	(+)	(-)
$\beta_\xi/\mu_\xi$	$4.64 \pm 0.25$	$-4.92 \pm 0.12$	$3.76 \pm 0.28$	$-4.11 \pm 0.31$
$\beta_\sigma/\mu_\sigma$	$4.31 \pm 0.20$	$-4.88 \pm 0.17$	$3.55 \pm 0.20$	$-3.61 \pm 0.23$
$\langle \beta/\mu \rangle$	$4.47 \pm 0.22$	$-4.90 \pm 0.15$	$3.66 \pm 0.24$	$-3.86 \pm 0.27$
$\beta_\xi/\mu_\xi - \beta_\sigma/\mu_\sigma$	$0.33 \pm 0.45$	$-0.04 \pm 0.29$	$0.21 \pm 0.48$	$-0.50 \pm 0.54$
$1/\beta_\xi$	$0.0452 \pm 0.0040$	$0.0673 \pm 0.0035$	$0.0481 \pm 0.0056$	$0.0922 \pm 0.0086$
$\beta_\sigma/\mu_\sigma^2$	$9.1 \pm 0.5$	$13.4 \pm 0.7$	$10.4 \pm 1.4$	$16.4 \pm 0.9$
$\beta_\xi$	$22.1 \pm 2.0$	$14.9 \pm 0.8$	$20.8 \pm 2.4$	$10.8 \pm 1.0$
$\beta_\sigma$	$2.04 \pm 0.31$	$1.77 \pm 0.21$	$1.22 \pm 0.31$	$0.79 \pm 0.14$
$\mu_\xi$	$4.77 \pm 0.68$	$-3.02 \pm 0.23$	$5.53 \pm 1.06$	$-2.64 \pm 0.45$
$\mu_\sigma$	$0.47 \pm 0.05$	$-0.36 \pm 0.03$	$0.34 \pm 0.07$	$-0.22 \pm 0.03$

vorticity fluctuations displays a scattering of the same order of magnitude than angular velocity fluctuations. Once again, an average over the bulk allows to measure  $\beta_\sigma/\mu_\sigma^2$ . We conclude that, for these von Kármán flow, the variances of azimuthal velocity and vorticity are constant in the flow bulk. This result is compatible with the mean field analysis drawn in the first part of this Letter for a Beltrami flow. Combining the two sets of results described above, we can independently evaluate  $(\mu_\sigma, \beta_\sigma)$  and  $(\mu_\xi, \beta_\xi)$ . Standard error estimates are typically 10%, ranging from 5 to 20%. Table I shows that these two couples are not equal to each other and even differ by one order of magnitude. This result is discussed in the next section.

*Conclusion.-* We have derived predictions concerning the mean flow and the fluctuations in an axisymmetric Euler-Beltrami flow using tools borrowed from statistical mechanics. These predictions, and especially the uniformity of the variances of  $u_\theta$  and  $\omega_\theta$  (Eqs. 8), have then been experimentally confirmed in the specific case of a turbulent von Kármán flow at large Reynolds number. This result is a priori unexpected since the theory, issued from the Euler equation, does not explicitly take into account the forcing and the dissipation which *implicitly* determine the form of the steady state. This is an additional confirmation that out of equilibrium steady states of a real turbulent flow may be described as equilibrium states of the Euler equation as suggested in [10]. Additionally, these relations provide two different values for an effective statistical temperature  $1/\beta$  of our system depending on the selected variable. Such non-uniqueness of statistical temperature in out of equilibrium systems has already been encountered in the context of glassy systems [12]. Turbulent flows may be another example of this out of equilibrium property. Meanwhile, one could possibly use correlation with hydrodynamics properties (such as variation with forcing, fluctuation rate or Reynolds number [13]) to decide whether one of the temperatures we measure is more relevant than the other to stand for a statistical temperature of the turbulence. Finally, in order

TABLE I: Non-dimensionalized statistical coefficients measured in our experiments following Eqs. (2) and (8) for the four forcings studied (two impellers, two senses). Raw measurements (lines 1-2 and 5-6) allow to calculate a Beltrami factor (line 3-4) and statistical coefficients (lines 7-10). Errors are calculated with standard 68% confidence intervals as the sum of the error on data fits (see Figs. 1 and 2) and of the statistical dispersion over the different runs. Each measurement is an average over 5 to 7 experiments performed at high  $Re$  between 1.2 and  $5 \times 10^5$ .

to test further the physical relevance of the FDR analogy, one should perform direct measurements of response functions as suggested by the *r.h.s.* of Eqs. (9). This is a yet unresolved and challenging experimental issue.

This work was supported by ANR TSF NT05-1-41492.

- 
- [1] L. F. Cugliandolo and J. Kurchan, Phys. Rev. Lett. **71**, 173 (1993); L. F. Cugliandolo *et al*, Phys. Rev. E **55**, 3898 (1997); J.-P. Bouchaud *et al.*, in *Spin Glasses and Random Fields*, edited by A. P. Young (World scientific, Singapore, 1997).
  - [2] L. Buisson *et al.*, Europhys. Lett. **63**, 603 (2003); D. Hérisson and M. Ocio, Eur. Phys. J. B **40**, 283 (2004).
  - [3] D. J. Evans *et al.*, Phys. Rev. Lett. **71**, 2401 (1993); G. Gallavotti and E. G. D. Cohen, Phys. Rev. Lett. **74**, 2694 (1995); C. Jarzynski, Phys. Rev. Lett. **78**, 2690 (1997); G. E. Crooks, Phys. Rev. E **60**, 2721 (1999).
  - [4] R. van Zon *et al.*, Phys. Rev. Lett. **92**, 130601 (2004); S. Ciliberto *et al.*, Physica A **340**, 240 (2004).
  - [5] L. Onsager, Nuovo Cimento (Supplemento) (1949).
  - [6] P.-H. Chavanis, Physica D **200**, 257 (2004).
  - [7] N. Leprovost *et al.*, Phys. Rev. E **73**, 046308 (2006).
  - [8] J. Sommeria and R. Robert, J. Fluid Mech. **229**, 291 (1991); J. Miller, Phys. Rev. Lett. **65**, 2137 (1990).
  - [9] R. Ellis *et al.*, Nonlin. **15** (2002) 239.
  - [10] R. Monchaux *et al.*, Phys. Rev. Lett. **96**, 124502 (2006).
  - [11] R. Monchaux, Ph.D. thesis, Université Diderot, Paris 7, 2007.
  - [12] S. Fielding and P. Sollich, Phys. Rev. Lett. **88**, 050603 (2002).
  - [13] It has already been shown that a local value of  $\overline{u_\theta^2} - \overline{u_\theta}^2$  behaves as  $(Re - 330)^{1/2}$  and saturates above  $Re = 3300$  for TM60 (-), F. Ravelet, A. Chiffaudel, and F. Daviaud, J. Fluid Mech. **601**, 339 (2008).
  - [14]  $\overline{x}$  stands for statistical average of  $x$ . Its experimental estimate is made by time-averaging assuming ergodicity.
  - [15] For a statistical equilibrium state of the 2D Euler equation, with general  $\overline{\omega} = f(\psi)$  relationship, one can derive  $\overline{\omega^2} - \overline{\omega}^2 = (1/\beta)d\overline{\omega}/d\psi$  [6] which is analogous to a FDR since it links the fluctuations of  $\omega$  to the temperature  $1/\beta$  and the susceptibility  $\chi = d\overline{\omega}/d\psi$ . This relation is the counterpart of Eq. (8b). 2D velocity  $\mathbf{v} = \nabla \times (\psi \mathbf{e}_z)$  can be written  $\mathbf{v} = \chi^{-1} \nabla \times (\overline{\omega} \mathbf{e}_z)$  which is the counter-

part of Eq. (7).